

Evanescent-Wave Trapping and Evaporative Cooling of an Atomic Gas at the Crossover to Two Dimensions

M. Hammes, D. Rychtarik, B. Engeser, H.-C. Nägerl, and R. Grimm

Institut für Experimentalphysik, Universität Innsbruck, Technikerstraße 25, A-6020 Innsbruck, Austria

(Received 16 August 2002; published 29 April 2003)

A dense gas of cesium atoms at the crossover to two dimensions is prepared in a highly anisotropic surface trap that is realized with two evanescent light waves. Temperatures as low as 100 nK are reached with 20 000 atoms at a phase-space density close to 0.1. The lowest quantum state in the tightly confined direction is populated by more than 60%. The system provides atoms at a mean distance from the surface as low as 1 μm , and offers intriguing prospects for future experiments on degenerate quantum gases in two dimensions.

DOI: 10.1103/PhysRevLett.90.173001

PACS numbers: 32.80.Pj, 03.75.-b, 34.50.-s

Systems with reduced dimensionality have attracted considerable attention in various areas of physics as they exhibit strikingly different properties in comparison to the three-dimensional case. A two-dimensional gas of ultracold atoms is realized when an anisotropic external trapping potential confines the motion to the lowest quantum state in one dimension and a weakly confined two-dimensional (2D) motion takes place in a plane. The crossover to two dimensions is reached when the thermal energy is reduced to values below the vibrational energy quantum in the tightly confined direction.

In the field of atomic quantum gases, there has been long-standing interest in two-dimensional systems in view of the phase transition to a quantum-degenerate gas [1], the onset of coherence [2], and modifications of interaction properties [3]. Spin-polarized hydrogen on a liquid-helium surface represents a 2D quantum gas as the adsorbed atoms occupy a single quantum state [4], and evidence of quantum degeneracy has been obtained [5]. The required cryogenic setup and the lack of efficient optical diagnostics, however, make detailed experimental studies on 2D gases of hydrogen very difficult, and thus there is great interest to realize analogous systems by using more readily accessible laser-manipulated atoms.

Few experiments with laser-cooled atoms have thus far approached 2D. In standing-wave traps, conditions were obtained with the predominant population of the lowest quantum state in one dimension [6–8]. In such traps, however, many individual traps are populated simultaneously so that phenomena related to individual systems are hardly accessible. Another approach is an anisotropic optical trap made of an elliptically focused laser beam and loaded with a Bose-Einstein condensate [9]; this trap, however, is diffraction limited and thus provides relatively small level spacing. Optical surface traps combine tight confinement in one direction with a single potential well. Recent surface trapping experiments [10,11] have approached 2D by populating a few bound states, yet far away from quantum degeneracy.

In this Letter, we report on trapping and evaporative cooling of a dense gas of Cs atoms in a double evanescent-wave trap (DEW trap, see illustration in Fig. 1). The trap was suggested by Ovchinnikov, Shul'ga, and Balykin already in 1991 [12] and has attracted considerable interest for various applications [13]. Its experimental realization, however, had to await the development of efficient surface trapping tools to accomplish loading of atoms into a narrow potential well very close to the surface. In general, the recent advances in integrated atom optics [14] have stimulated considerable interest in the subject of cold atoms close to a surface. While present magnetic approaches to trap atoms close to surfaces encounter limitations by surface effects at distances of a few 10 μm [15], our optical approach readily provides a dense atomic sample as close as 1 μm to the surface and thus offers intriguing new possibilities for experiments on atom-surface interactions and the micromanipulation of atoms.

The DEW trap relies on the optical dipole force in a combination of a repulsive and an attractive EW field, produced on the surface of a dielectric prism by total internal reflection of two laser beams. The two fields with

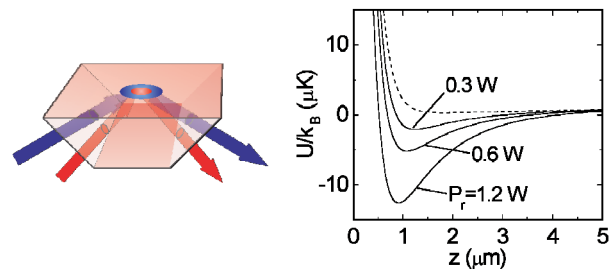


FIG. 1 (color online). Illustration of the DEW trap and calculated potentials normal to the surface in the trap center. The attractive van-der-Waals part at short distances is not shown. The solid lines refer to different values of the laser power P_r of the attractive EW. The dashed line shows the potential for $P_r = 0$.

wavelengths λ_i ($i = r, b$) are created by laser sources tuned below and above the atomic transition (red and blue detuning), respectively. Normal to the surface, the two fields decay exponentially with characteristic lengths of $\Lambda_i = \lambda_i/2\pi \times (n^2 \sin^2 \theta_i - 1)^{-1/2}$, determined by the angle of incidence θ_i , the optical wavelength λ_i , and the refractive index n . A narrow, wavelength-sized potential well is created close to the surface when the decay length Λ_b of the repulsive EW is short compared to Λ_r of the attractive field. This is reached by setting the red-detuned laser beam near to the critical angle $\theta_c = \arcsin(1/n)$ of total internal reflection and the blue one much further away. Typical angles are $\theta_r - \theta_c$ of a few tens of a degree and $\theta_b - \theta_c$ of a few degrees. In addition to tight confinement normal to the surface, lateral confinement is achieved when the laser beam used for the attractive EW has a smaller diameter than the one used for the repulsive field.

In our experiment, the repulsive EW is generated with the beam of a Ti:sapphire laser at a wavelength of $\lambda_b = 850.5$ nm (1.6 nm blue detuning with respect to the Cs D_2 line at 852.1 nm). The angle of incidence is set to $\theta_b = 46.8^\circ$, i.e., 3.2° above the critical angle of the fused-silica prism ($n = 1.45$). The beam for the attractive EW is derived from an Yb-fiber laser with $\lambda_r = 1064$ nm and set to 0.2° above θ_c . The resulting decay lengths are $\Lambda_b = 395$ nm and $\Lambda_r = 2.0$ μm . The beams are focused to waists of $w_b = 400$ μm and $w_r = 160$ μm .

The total trap potential can be written as

$$U(\mathbf{r}) = U_b(x, y)e^{-2z/\Lambda_b} - U_r(x, y)e^{-2z/\Lambda_r} - \alpha_{\text{vdW}}z^{-3}(1 + 2\pi z/\lambda_{\text{eff}})^{-1} + mgz, \quad (1)$$

where $U_i(x, y) = \hat{U}_i \exp(-2x^2/w_i^2 - 2y^2/w_i^2 \cos^2 \theta_i)$ are the optical potentials directly at the surface ($z = 0$). For the maximum potentials in the center of the trap, we calculate $\hat{U}_b/k_B = 325$ μK and $\hat{U}_r/k_B = 43$ μK at typical beam powers of $P_b = 1.15$ W and $P_r = 1.2$ W, respectively; k_B denotes Boltzmann's constant. The laser beams are linearly polarized in the plane of incidence (TM polarization) to maximize the EW field. The van der Waals surface attraction [16,17], which is described by the third term in Eq. (1) [18], plays a minor role in our experiment. The gravitational potential is represented by the last term in Eq. (1) with m denoting the Cs atom's mass and g the gravitational acceleration.

Figure 1 shows the calculated potential in the center of the trap ($x, y = 0$). For $P_r = 1.2$ W, the power that we use for loading, a 13 μK deep well is realized with its minimum located 0.9 μm away from the surface. For decreasing power of the attractive EW, the well becomes shallower and the minimum moves away from the surface. Without attractive EW (dashed line), the vertical motion is still confined because of gravity, but without any horizontal confinement.

The multistage loading sequence proceeds as follows: Atoms are released from a magneto-optical trap (MOT)

into the gravito-optical surface trap (GOST) of Ref. [20], where an unpolarized sample in the lower hyperfine state ($F = 3$) is produced by evanescent-wave Sisyphus cooling. A part of the atoms is then transferred through elastic collisions into a narrow, far-detuned intense laser beam perpendicularly intersecting the evanescent wave in the center of the GOST [20]; this beam has a Gaussian beam waist of 160 μm and is derived with an initial power of 7.2 W from the same Yb-fiber laser that later produces the attractive field of the DEW trap. The repulsive evanescent wave applied at this stage is already the one that is later used in the DEW trap. The sample is then further cooled adiabatically and evaporatively by exponentially ramping down the power of the horizontally confining beam to 2 W in 2 s. In this way, we obtain our surface reservoir of 1.8×10^6 atoms at 3.0 μK , corresponding to a peak number density of $\sim 10^{13}$ cm^{-3} and a peak phase-space density of $\sim 10^{-3}$ [21].

Transfer into the DEW trap from the reservoir is then accomplished in a time interval of 50 ms by ramping down the power of the red-detuned beam from 2 W to zero simultaneously with ramping up the power of the attractive EW from zero to the optimum loading power $P_r = 1.2$ W. The lateral confinement of the reservoir beam and the DEW trap are approximately matched, so that the loading process is governed by the vertical motion. Up to 10^5 atoms are observed in the DEW trap after 150 ms when the unbound atoms remaining from the reservoir have laterally escaped. Measurements of the atom number are performed via fluorescence images after recapture into the MOT [19,20].

The vertical trap frequency ν_z , which corresponds to the vibrational energy quantum $h\nu_z$ in the tightly confined direction, is measured by parametric excitation [22]. After loading the DEW trap under fixed conditions ($P_r = 1.2$ W), we ramp P_r to a variable value in 50 ms and apply a sinusoidal power modulation with a typical depth of 10% to the repulsive EW for 150 ms. We then wait 100 ms to let unbound atoms escape and measure the number of remaining atoms. A typical trap-frequency measurement is shown in Fig. 2(a) for $P_r = 0.9$ W; it exhibits clear minima at the trap frequency and its second

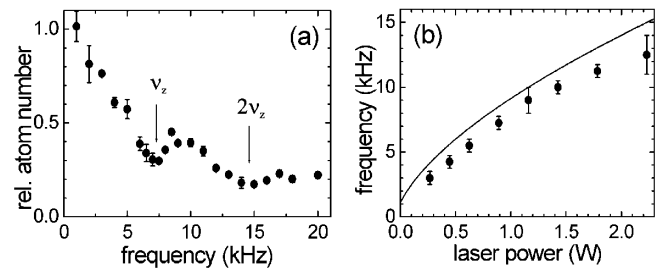


FIG. 2. Measurements of the trap frequency in the tightly confined z direction. (a) Fraction of atoms remaining trapped for $P_r = 0.9$ W after 150 ms of parametric excitation at a variable frequency. (b) Measured trap frequency versus P_r in comparison with a calculation based on Eq. (1).

harmonics. Figure 2(b) shows the measured values for the trap frequency in comparison with the results of a calculation according to Eq. (1); the latter is based on a harmonic approximation to the minimum of the trap potential $U(\mathbf{r})$ which we calculate for our experimental conditions without any adjustable parameter. The measurements are affected by the lateral thermal spread of the sample and by anharmonicities of the trap and therefore show a sample-averaged frequency which is slightly below the frequencies in the trap center. If this minor deviation is taken into account, the measurements well confirm the theoretical frequencies. At $P_r = 1.2$ W, we calculate a vertical trap frequency of 10.2 kHz and a mean horizontal frequency of 50 Hz. The typical aspect ratio of the trap is thus of the order of 200.

The temperature of the sample is measured with a release-and-recapture method. Both EW fields are turned off simultaneously by acousto-optical modulators. The sample then undergoes a ballistic expansion in the field of gravity and atoms hitting the room-temperature surface are immediately lost. After a short release time, the repulsive EW is turned on again to prevent further atoms from hitting the surface, and the number of remaining atoms is measured in the standard way by recapture into the MOT. A theoretical model based on the assumption of a thermal distribution in the known trap potential is then used to fit the data with a single parameter and thus to accurately determine the mean kinetic energy of the released sample. At temperatures down to a few 100 nK, a classical approximation holds and the model directly provides the temperature. At lower temperatures, quantum corrections due to the zero-point energy and the discrete level spacing can be introduced within a simple harmonic oscillator model; for all measurements presented here, these corrections stay well below 20%. Figure 3 shows two examples of temperature measurements obtained for a “hot” ($2.7 \mu\text{K}$) and a “cold” (100 nK) sample.

We implement forced evaporative cooling by ramping down the power P_r of the attractive EW. This introduces two-dimensional evaporation, as energetic atoms

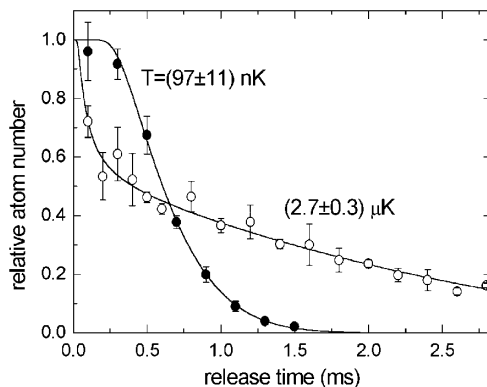


FIG. 3. Temperature measurements in the DEW trap after 300 ms of storage at constant trap depth (○) and after forced evaporative cooling (●).

escape horizontally from the trap. In the vertical direction, no evaporation can take place because of gravity. Our scheme decompresses the sample and provides simultaneous adiabatic and evaporative cooling with a drastic reduction of the temperature T . The applied release-and-recapture thermometry, strictly speaking, yields a vertical temperature which does not necessarily equal the horizontal one [19]. However, because of a rapid collisional thermalization and the fact that cooling occurs as a result of horizontal selection, the vertically measured T in general provides a reasonable measure for the horizontal temperature.

The evaporation ramp is started immediately after the DEW trap is loaded and the red-detuned transfer beam is extinguished. The power of the attractive EW is exponentially reduced according to $P_r(t_{\text{ev}}) = P_0 \exp(-t_{\text{ev}}/\tau)$ with $P_0 = 1.2$ W; the time constant $\tau = 120$ ms is found to provide optimum cooling results. Data are taken for evaporation times t_{ev} between 150 and 450 ms. For shorter times, reliable measurements are not possible because untrapped reservoir atoms have not fully disappeared after release from the transfer beam. The two solid lines in Fig. 4 (upper graph) show the reduction of the trap depth $\hat{U}(t_{\text{ev}})$ and the corresponding slower decrease of the vibrational level spacing $h\nu_z(t_{\text{ev}})$, as calculated from the potential according to Eq. (1). For all our measurements, the trap fulfills $h\nu_z \ll \hat{U}$ and stays in a quasiclassical regime with at least a few bound states of the vertical motion.

The experimental data in Fig. 4 show the observed evaporation process. For t_{ev} between 150 and 300 ms, the trapped atom number N decays exponentially by a total factor of about 3. In this time interval, the temperature

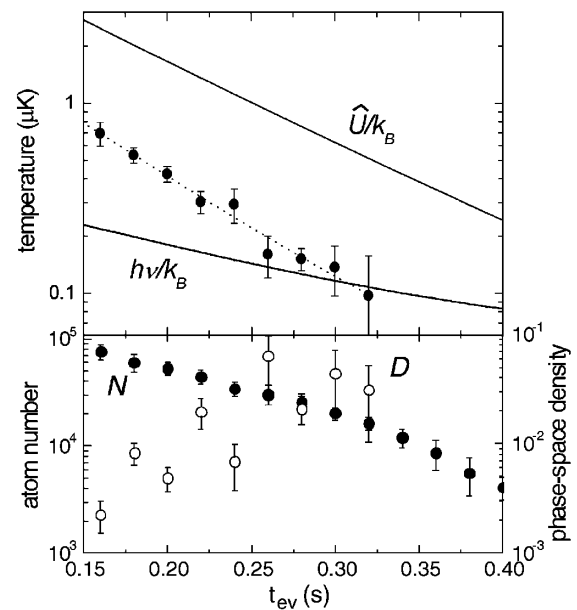


FIG. 4. Evaporative cooling in the DEW trap. Upper graph, temperature T versus evaporation time t_{ev} in comparison with the trap depth \hat{U} and the vibrational quantum $h\nu_z$. Lower graph, atom number N and phase-space density D .

drops from 800 to 100 nK in a way approximately proportional to the trap depth ($k_B T \approx \eta \hat{U}$). The corresponding truncation parameter that characterizes the evaporation is $\eta \approx 5$. The phase-space density D [21] of the sample increases by almost 2 orders of magnitude from $\sim 10^{-3}$ to values close to 0.1. This observed evaporation process is readily understood in terms of standard evaporation theory [23] with both the truncation parameter $\eta \approx 5$ and the time scale of the evaporation fitting well to the model. The calculated time scale τ_{el} for elastic collisions [24] varies between 4 ms ($\tau_{ev} = 150$ ms) and 10 ms (300 ms), and the corresponding evaporation time scale of $\sqrt{2}\eta^{-1}e^{\eta}\tau_{el} \approx 40\tau_{el}$ agrees with the time constant of the applied evaporation ramp. For longer evaporation ($t_{ev} \geq 300$ ms), a faster loss of atoms is observed and indicates a breakdown of the evaporation process. Because of the low atom number, temperature measurements are no longer possible.

The crossover to a 2D gas is realized for $t_{ev} \approx 300$ ms when $k_B T$ reaches the vibrational energy quantum $h\nu_z$ of the tightly confined vertical motion. In a harmonic approximation, the condition $k_B T = h\nu_z$ corresponds to a mean vibrational quantum number of $\bar{n} = 0.58$ and a ground-state population of 63%. This, together with the highest attained phase-space densities of the order of 0.1 [21], highlights the potential of the trap for future experiments on degenerate quantum gases in two dimensions.

Our experiment is presently limited by the fact that, for low temperatures, the unpolarized Cs sample in the $F = 3$ ground state becomes unstable against inelastic two-body collisions [25]. At typical residual magnetic fields of ~ 10 mG, the mean internal energy per atom in a fully unpolarized sample is $k_B \times 500$ nK. For temperatures below this value, inelastic collisions can be expected to release this energy into the translational motion, which leads to heating and trap loss. We indeed observe that the evaporation efficiency critically depends on the compensation of Earth's magnetic field. We plan to overcome this limitation by polarizing the atoms into the lowest substate ($F = 3, m = 3$). Such a polarized sample is stable against two-body decay and, moreover, offers magnetic tunability of s -wave scattering by low-field Feshbach resonances [26]. Gravity can be compensated by using magnetic gradients so that atoms can evaporate three dimensionally out of the trap. With these modifications, quantum degeneracy of a 2D cesium gas may be reached under conditions where the DEW trap supports just a single vertical bound state. This would constitute a unique system with strong analogies to H on liquid He, but with full optical access and magnetically tunable interactions.

In conclusion, we have realized a cold and dense gas of Cs atoms in a highly anisotropic optical trap situated very close to a dielectric surface. The trap provides a sample of $\sim 10^5$ atoms at a mean distance of about $1 \mu\text{m}$ from the surface, much closer than in any other trapping scheme. A particular application consists in experiments on 2D quantum gases. By evaporative cooling, we have reached

temperatures as low as 100 nK and conditions at the crossover to two dimensions. The system offers intriguing prospects for future research on degenerate quantum gases in two dimensions.

We gratefully acknowledge support by the Austrian Science Fund (FWF) within SFB 15 (project part 15).

-
- [1] V. Bagnato and D. Kleppner, Phys. Rev. A **44**, 7439 (1991).
 - [2] Y. Kagan, B. Svistunov, and G. Shlyapnikov, Sov. Phys. JETP **66**, 314 (1987).
 - [3] D. Petrov, M. Holzmann, and G. Shlyapnikov, Phys. Rev. Lett. **84**, 2551 (2000).
 - [4] J.T.M. Walraven, in *Fundamental Systems in Quantum Optics*, edited by J. Dalibard, J.M. Raimond, and J. Zinn-Justin (Elsevier, Amsterdam, 1992), p. 485.
 - [5] A. Safonov *et al.*, Phys. Rev. Lett. **81**, 4545 (1998).
 - [6] V. Vuletić, C. Chin, A.J. Kerman, and S. Chu, Phys. Rev. Lett. **81**, 5768 (1998).
 - [7] I. Bouchoule *et al.*, Phys. Rev. A **59**, 8(R) (1999).
 - [8] I. Bouchoule, M. Morinaga, C. Salomon, and D. Petrov, Phys. Rev. A **65**, 033402 (2002).
 - [9] A. Görlitz *et al.*, Phys. Rev. Lett. **87**, 130402 (2001).
 - [10] H. Gauck *et al.*, Phys. Rev. Lett. **81**, 5298 (1998).
 - [11] M. Hammes, D. Rychtarik, and R. Grimm, C.R. Acad. Sci. Ser. IV **2**, 625 (2001).
 - [12] Yu. B. Ovchinnikov, S. Shul'ga, and V. Balykin, J. Phys. B **24**, 3173 (1991).
 - [13] H. Mabuchi and H. Kimble, Opt. Lett. **19**, 749 (1994); P. Desbiolles and J. Dalibard, Opt. Commun. **132**, 540 (1996); A.H. Barnett *et al.*, Phys. Rev. A **61**, 023608 (2000); P. Domokos and H. Ritsch, Europhys. Lett. **54**, 306 (2001); Y. Colombe *et al.*, J. Opt. B: Quantum Semiclass. Opt. **5**, S155 (2003); J.P. Burke *et al.*, Phys. Rev. A **65**, 043411 (2002); R. Côté and B. Segev (to be published).
 - [14] H. Ott *et al.*, Phys. Rev. Lett. **87**, 230401 (2001); W. Hänsel, P. Hommelhoff, T.W. Hänsch, and J. Reichel, Nature (London) **413**, 498 (2001).
 - [15] J. Fortagh *et al.*, Phys. Rev. A **66**, 041604(R) (2002).
 - [16] A. Landragin *et al.*, Phys. Rev. Lett. **77**, 1464 (1996).
 - [17] F. Shimizu, Phys. Rev. Lett. **86**, 987 (2001).
 - [18] $\alpha_{vdW} = 5.8 \times 10^{-49} \text{ kg m}^5 \text{ s}^{-2}$, $\lambda_{\text{eff}} = 907 \text{ nm}$.
 - [19] Yu. B. Ovchinnikov, I. Manek, and R. Grimm, Phys. Rev. Lett. **79**, 2225 (1997).
 - [20] M. Hammes, D. Rychtarik, H.-C. Nägerl, and R. Grimm, Phys. Rev. A **66**, 051401(R) (2002).
 - [21] Phase-space densities are calculated assuming a fully unpolarized sample in $F = 3$.
 - [22] S. Friebe *et al.*, Phys. Rev. A **57**, 20(R) (1998).
 - [23] W. Ketterle and N.J. van Druten, Adv. At. Mol. Opt. Phys. **37**, 181 (1996).
 - [24] We use a scattering cross section of $\sigma = 4\pi(800a_0)^2$ (a_0 is Bohr's radius) as a reasonable assumption regarding the resonant scattering properties of Cs.
 - [25] D. Guéry-Odelin, J. Söding, P. Desbiolles, and J. Dalibard, Europhys. Lett. **44**, 26 (1998).
 - [26] A. Kerman *et al.*, C.R. Acad. Sci. Ser. IV **2**, 633 (2001).